Liquid Crystals
Publication details, including instructions for authors and subscription information:
http://www.informaworld.com/smpp/title~content=t713926090

Thermodynamic modelling of carbonaceous mesophase mixtures

Mojdeh Golmohammadi[a]; Alejandro D. Rey[a]
[a] Department of Chemical Engineering, McGill University, Montreal (Quebec) H3A 2B2, Canada

To cite this Article Golmohammadi, Mojdeh and Rey, Alejandro D.(2009) 'Thermodynamic modelling of carbonaceous mesophase mixtures', Liquid Crystals, 36: 1, 75 — 92
To link to this Article: DOI: 10.1080/02678290802666218
URL: http://dx.doi.org/10.1080/02678290802666218

Liquid Crystals,
Vol. 36, No. 1, January 2009, 75–92

Taylor & Francis
Taylor & Francis Group

Thermodynamic modelling of carbonaceous mesophase mixtures

Mojdeh Golmohammadi and Alejandro D. Rey*

Department of Chemical Engineering, McGill University, Montreal (Quebec) H3A 2B2, Canada

(Received 19 October 2008; final form 4 December 2008)

The Maier–Saupe model is extended to the binary mixtures of uniaxial discotic nematogens to compute the equilibrium phase diagrams of carbonaceous mesophases. The ordering in the mixture is affected by temperature (thermotropic) and concentration (lyotropic). The magnitude of molecular weight asymmetry of two nematogens and the strength of molecular interaction control the type of mixture: (a) non-ideal mixtures arise under sufficiently weak interaction and lower molecular weight differences; and (b) ideal mixtures arise under stronger molecular interaction and higher molecular weight asymmetries. Ideal mixtures have clearing temperatures that change monotonically with concentration and the higher molecular weight component has higher-order parameter. Non-ideal mixtures have a minimum in the clearing temperature at a critical concentration at which the binary mixture behaves like a pure nematogen and the ordering of the two species are identical; for non-ideal mixtures the relative magnitude in the species' ordering depends on the concentration; the species with lower molecular weight can have a higher order if its concentration is high enough. Characterisation protocols based on X-ray computations and direct methods are proposed to detect the type of mixture and the magnitude of molecular interaction. The results provide new tools to design carbon fibres based on molecular properties.

Keywords: discotic nematic liquid crystals; carbonaceous mesophase; mixture; molecular weight; concentration; lytropic; thermotropic; X-ray

1. Introduction

Carbonaceous mesophases (CMs), first reported by Brooks and Taylor (*1*), are discotic nematic liquid crystalline (DNLC) mixtures obtained from petroleum pitches and synthetic naphthalene precursors (*2*). The composition, polydispersity and molecular orientation of CMs play a significant role on the final properties of cokes (*3*), carbon foams, carbon/carbon composites (*4*) and carbon fibres (*5–8*). Property optimisation and cost reduction of high-performance carbonaceous materials require a better understanding of the thermodynamics, and dynamics of CM mixtures and their intrinsic properties. For instance, it is known that the final structure of the fibres based on the pure liquid crystalline materials are influenced by the temperature (*9*); however, in reality CMs are not pure liquid crystals (LCs), they are composed of the species with different molecular weights and concentrations. Several theoretical and experimental studies have been carried out on binary nematic liquid crystalline (NLC) mixtures (*8, 10–14*). However, no systematic investigation has been performed to find out how the nature of the mixture and its composition control the final structure of the CM fibres and optimise product performance in structural and functional (thermal) applications. To meet this objective this paper focuses on the equilibrium thermodynamics of CM binary mixtures. As a starting point in this weakly explored area, we consider an athermal solution of two thermotropic uniaxial discotic nematogens that only differ in molecular weight thus precluding phase separation. It has been shown previously in the literature that phase separation does not play a significant role in the mixture of nematic LCs differing in molecular weight. The components of some of the mixtures that have been investigated also differ in the chemical structure (*12, 15–17*). Based on available experimental data (*10*) we choose representative molecular weights of 200 to 1400.

The theory derived in this work can also be used in other NLC areas. For instance, mixtures of two or more mesogens are also important in liquid crystal display (LCD) applications, where composition of the mixture is used to overcome the restrictions owing to thermal operating conditions and optimisation of the response time by the calibration of viscoelastic properties. The Maier–Saupe (MS) theory is widely used to describe the thermodynamics of nematic LCs (*18*). This mean field theory gives the temperature-dependence of the molecular orientation in mesogenic materials. It predicts the values of the experimentally measured scalar order parameters (*19*) very well and hence it has been applied to different NLC systems and can be adjusted to their mixtures (*12, 20*). In this paper we use the MS theory adjusted to binary uniaxial discotic nematogens.

*Corresponding author. Email: alejandro.rey@mcgill.ca

ISSN 0267-8292 print/ISSN 1366-5855 online

DOI: 10.1080/02678290802666218
http://www.informaworld.com

The usual description of a single species discotic nematic LC (*21*) is based on the normalised orientation distribution function ODF(**u**), where **u** is the orientation of the disc normal, given by

$$\mathrm{ODF}(\mathbf{u}) = \frac{1}{2\pi} f_{\mathrm{o}} + \frac{3\times 5}{2\pi\times 2} Q_{ij}^2 f_{ij}^2 + \frac{3\times 5\times 7\times 9}{2\pi\times 2\times 3\times 4} Q_{ij}^4 f_{ij}^4 + \cdots \tag{1}$$

where $f_{\mathrm{o}}, f_{ij}^2, f_{ijkl}^4, \ldots$ are orthogonal surface spherical harmonics and where the coefficients of the Fourier expansion, $\mathbf{Q}^2$, $\mathbf{Q}^4$,... are symmetric and traceless tensors found using orthogonality. The quadrupolar tensor order parameter $\mathbf{Q}^2$ used in the Landau–de Gennes viscoelastic model (*22*) is

$$\mathbf{Q} \equiv \mathbf{Q}^2 = \int_{\mathbb{Z}^2} \mathrm{f}(\mathbf{u})\mathbf{f}^2 \, dA = \int_{\mathbb{Z}^2} \mathrm{f}(\mathbf{u}) \left(\mathbf{uu} - \frac{\boldsymbol{\delta}}{3} \right) \quad dA = \left\langle \mathbf{uu} - \frac{\delta}{3} \right\rangle \tag{2}$$

where $\mathbb{Z}^2$ is half the unit sphere. For uniaxial phases **Q** is given in terms of a temperature-dependent scalar order parameter $s(T)$ and the average molecular orientation or director **n**: $\mathbf{Q}=\mathrm{s}(\mathbf{nn}-\mathbf{I}/3)$. The possible states of uniaxial discs are: (i) isotropic (I), $\mathrm{s}=0$; and (ii) nematic, $\mathrm{s}>0$. For CMs at high temperatures the stable phase is isotropic and at sufficiently lower temperatures it is nematic; issues of stability of nematic phases in CMs are discussed in (*23*). As shown in Appendix 2 (Equation (36)), for binary mixtures of uniaxial mesogens, a similar development leads to the mixture quadrupolar order parameter:

$$\mathbf{Q}_{\mathrm{mix}} \equiv \mathbf{Q} = m_1\mathbf{Q}_1 + m_2\mathbf{Q}_2 \tag{3}$$

where m_i is the mole fraction of ith component. For binary discotic nematogens at equilibrium we find collinear directors ($\mathbf{n}_1=\mathbf{n}_2$) and the mixture uniaxial scalar order parameter then is: $\mathrm{s}_{\mathrm{mix}}=\mathrm{m}_1\mathrm{s}_1+\mathrm{m}_2\mathrm{s}_2$. Nevertheless, since the ordering states of each species are coupled and are also dependent on temperature and dilution, we expect, based on the above observations, that binary mixtures display three states:

(i) isotropic (I), $\mathrm{s}_1=0$, $\mathrm{s}_2=0$;
(ii) nematic (N_{12}), with $\mathrm{s}_1 \geqslant \mathrm{s}_2$;
(iii) nematic (N_{21}), with $\mathrm{s}_1 \leqslant \mathrm{s}_2$.

For the exceptional case when $\mathrm{s}_1=\mathrm{s}_2$, the nematic mixture behaves like a single component system. Previous work (*24*) on liquid crystalline mixtures of dissimilar mesogens focuses on phase separation effects while this paper focuses on similar mesogens under no phase separation. Figure 1 shows a schematic of the possible equilibrium phase diagrams for binary CMs, in terms of temperature (T) as a function of composition (m_1). The diagrams show the equilibrium phases that are possible for different degrees of interaction (β) and different degrees of molecular weight difference between the two components (ΔM_{w}); in this example species '1' has higher molecular weight and, hence, nematic– isotropic (NI) transition temperature than species '2'. Figure 1(a) shows the thermodynamic phase diagram of a typical non-interacting ($\beta=0$) mixture. The two full lines denote the NI transition for each species; the decreasing transition temperature as dilution increases is the typical lyotropic effect. As the two transition lines cross, four phase regions are possible: I_1–I_2, I_1–N_2, I_2–N_1, N_1–N_2, where the subscripts 1 and 2 denote the species. For example, when $m_1=0.6$, quenching from a sufficiently high temperature leads to the following sequence:

$$\mathrm{I}_1, \mathrm{I}_2 \rightarrow \mathrm{N}_1, \mathrm{I}_2 \rightarrow \mathrm{N}_1, \mathrm{N}_2.$$

In the presence of molecular interaction ($\beta>0$), shown in Figures 1(b) and (c), the crossing transition lines become a single continuous isotropic–nematic (IN) transition curve, such that below (above) this curve the two species are in the nematic (isotropic) state. Depending on the nature of the mixture (i.e. molecular weight difference ΔM_{w} and the interaction β between the components) N_{21} can show up (Figure 1(c)) or it can disappear (Figure 1(b)). This fact is reflected in the temperature-concentration phase diagram of the mixtures (T, m_1), which can be classified as follows.

(i) The transition temperature, T_{NI}, increases monotonically by increasing concentration; this type of behaviour, which is called ideal, does not exhibit the N_{21} phase (Figure 1(b)). By decreasing the temperature the only possible transition when $M_{\mathrm{w1}}>M_{\mathrm{w2}}$ is

$$\mathrm{I}_1, \mathrm{I}_2 \rightarrow \mathrm{N}_1, \mathrm{N}_2$$

with $\mathrm{s}_1>\mathrm{s}_2$. The spheres below the diagram are schematics of the orientation distribution functions of the two components on the unit sphere, where the size of the white polar cap represents the degree of molecular order; since $s_1>s_2$ the white area of '1' is smaller than that for '2'.
(ii) The transition temperature exhibits a minimum by increasing the concentration. This type of behaviour, shown in Figure 1(c) is called non-ideal and allows the formation of the N_{21}

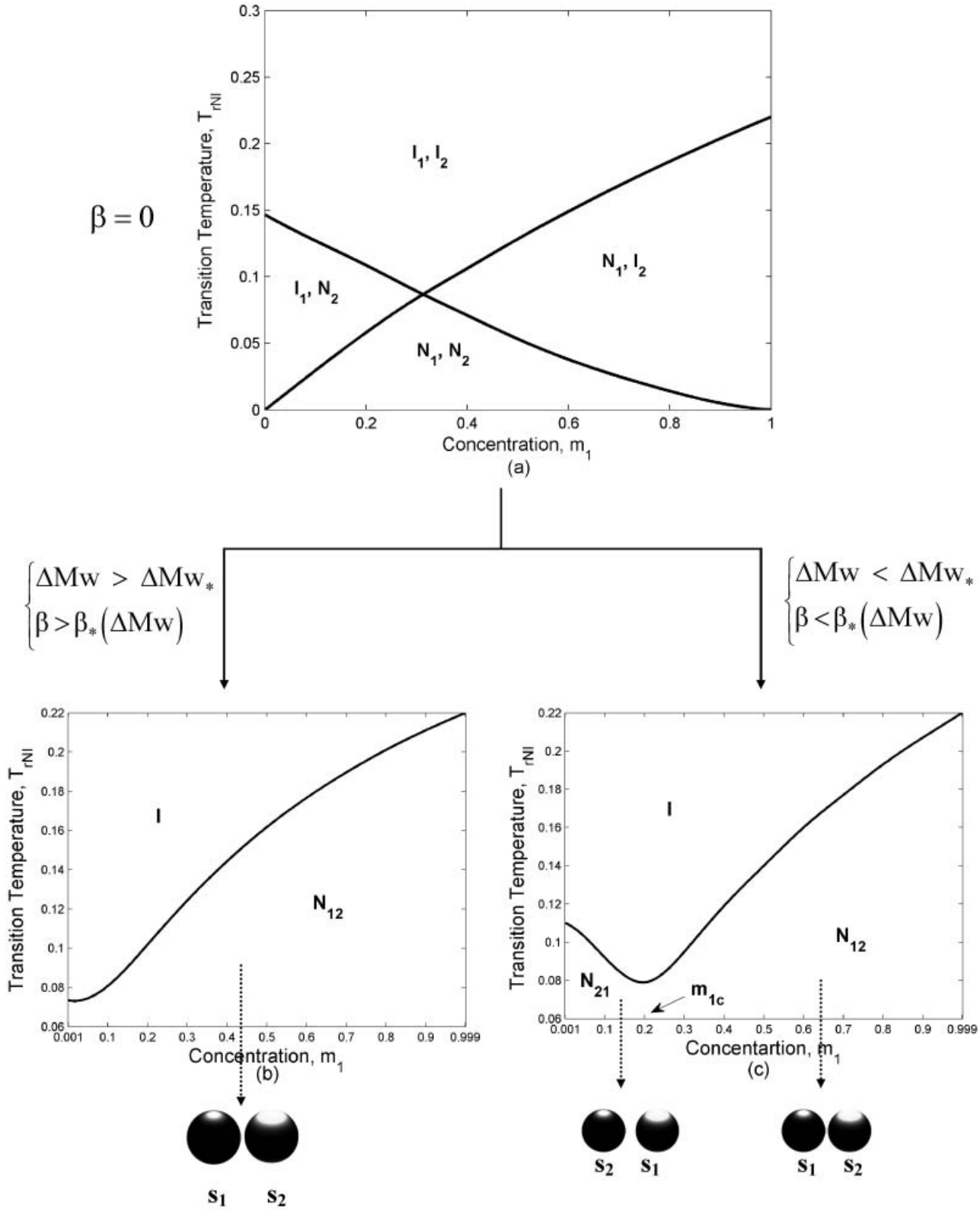

Figure 1. Schematics of the expected thermodynamic phase diagrams in terms of temperature as a function of composition: (a) for non-interacting mixtures ($\beta=0$); (b) for sufficiently strongly interacting mixtures and/or sufficiently large molecular weight asymmetry; (c) for weakly interacting mixtures and/or small molecular weight asymmetry.

mixture ($s_2 > s_1$) even though $M_{w2} < M_{w1}$. The N_{21} and N_{12} areas are separated by a vertical line that defines the critical concentration (m_{1c}) at which $s_1 = s_2$ and the binary mixture behaves as a single-component nematogen. The critical mixture that emerges due to concentration effects is characterised by the minimum transition temperature in the temperature-composition phase diagram (T, m_1). These mixtures are formed at a specific concentration; we call it the critical concentration, m_{1c}. Depending on the concentration values two cases arise:

(1) below the critical concentration, the low-molecular-weight component which has higher concentration is more ordered and, as a result, has a major contribution to the ordering of the mixture (lyotropic effect) so that $s_2 > s_1$ (N_{21}), as shown in the orientation distribution functions below the figure;
(2) for more concentrated systems (above critical concentration), the component with higher molecular weight makes the major ordering contribution to the mixture (M_w effect) so that $s_1 > s_2$ (N_{12}), as shown in the orientation distribution function below the figure.

The specific objectives of this paper are:

(i) to develop and solve an equilibrium thermodynamic model for binary discotic nematogens athermal mixture based on the MS model;
(ii) to characterise the role of intrinsic properties (molecular weight asymmetry, and molecular interactions) and dilution on the nematic structure;
(iii) to characterise phase transition and critical concentration in binary discotic nematogenic mixtures;
(iv) to derive an equation for the value of the interaction in the critical mixture;
(v) to propose methods to assess the magnitude of the interaction parameter and classify mixtures.

The main focus of the paper is to describe the effect of mixing, dilution, molecular weight asymmetry on the molecular order, and phase ordering and phase transition of the mixture. Analysis of heat of transitions and related thermodynamic aspects of phase transitions are outside the scope of this paper.

The organisation of this paper is as follows. Section 2 presents the MS binary mixture model; thermodynamic consistency and convergence to single-component expression is proven. The main parameters are identified and the numerical solution scheme is defined. The thermotropic and lyotropic nature of these mixtures is discussed and the effect of molecular weight is established. Section 3 presents the derivation of the equation used to characterise the interaction parameter β, as well as the derivation of the X-ray intensity to determine the type of the mixture as well as the value of the critical concentration. Section 4 presents the numerical results and discussion: Section 4.1 discusses the effect of (i) the relative alignment of the components, (ii) the molecular weight asymmetry, (iii) dilution and (iv) the interaction parameter on the molecular structure and ordering of the mixture. Section 4.2 discusses the effect of different parameters on the phase diagram of a CM binary mixture; as mentioned above the intrinsic parameters are molecular weight asymmetry (ΔM_w) and the interaction parameter (β) and the operating conditions are concentration (m_1) and temperature (T). Section 4.3 presents X-ray intensity and the average ordering at transition as the tools to characterise the type of the mixture as well as the value of the critical concentration. Section 5 provides the conclusions. Appendix 1 presents the single-component MS model in a form compatible with the mixture model. Appendix 2 derives the orientation distribution of a nematic mixture in terms of the single component distributions and derives the equation for the mixture quadrupolar order parameter $\mathbf{Q}_{mix}$.

2. Maier-Saupe binary mixture model

The MS model for a single-component nematic LC (*25*) is briefly described in Appendix 1 and extended below to a binary mixture of two discotic nematogens. For a homogeneous binary mixture, the internal energy E_{mix} per molecule is given by the summation of three contributions:

$$E_{mix} = E_{11} + E_{22} + E_{12} \tag{4}$$

due to self (1–1, 2–2) and cross (1–2) species interactions. Figure 2 shows a schematic of the

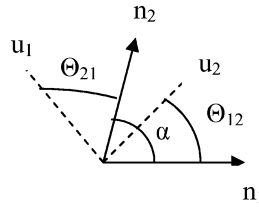

Figure 2. Schematic of molecular orientation ($\mathbf{u}_1$,$\mathbf{u}_2$) and directors ($\mathbf{n}_1$,$\mathbf{n}_2$) in binary discotic nematogens which form a single nematic phase. The relative angle between the directors is α.

components in the binary mixture, where $\mathbf{u}_1$ and $\mathbf{u}_2$ are molecular unit normals and $\mathbf{n}_1$ and $\mathbf{n}_2$ are the corresponding directors with the relative alignment α. In view of Equation (4), the internal energy of the mixture is (see Appendix 1) generalised to

$$E_{\mathrm{mix}}(\mathbf{Q}) = -\frac{3}{4} W_{11}\mathbf{Q}_1{:}\mathbf{Q}_1 - \frac{3}{4} W_{22}\mathbf{Q}_2{:}\mathbf{Q}_2 - \frac{3}{2} W_{12}\mathbf{Q}_1{:}\mathbf{Q}_2 \tag{5}$$

where the composition and molecular weight-dependent interaction parameters $\{W_{11}, W_{22}, W_{12}\}$ are:

$$\mathrm{W_{ii}} = \mathrm{m_i^2}\, U_{\mathrm{ii}};\ \mathrm{W_{12}} = \mathrm{m_1 m_2}\, U_{12};$$
$$U_{\mathrm{ii}} = \bar{U}_{\mathrm{ii}} \frac{M_{wi}}{\mathrm{m_1} M_{\mathrm{w1}} + \mathrm{m_2} M_{\mathrm{w2}}};$$
$$U_{12} = \bar{U}_{12} \frac{\sqrt{M_{\mathrm{w1}} M_{\mathrm{w2}}}}{\mathrm{m_1} M_{\mathrm{w1}} + \mathrm{m_2} M_{\mathrm{w2}}}$$

where $M_{\mathrm{w}i}$ denotes the molecular weight of the ith component, m_i its molar fraction and $\{\bar{\mathrm{U}}_{11}, \bar{\mathrm{U}}_{22}, \bar{\mathrm{U}}_{12}\}$ are the bare interaction parameters. Based on Equation (5) and the MS model, the partial internal potentials (Φ_1, Φ_2) acting on each species are

$$\Phi_1 = \frac{\partial \mathrm{E_{mix}}}{\partial \boldsymbol{Q}_1}{:}\left(\mathbf{u}_1\mathbf{u}_1 - \frac{\mathbf{I}}{3}\right) = -\frac{3}{2}(\mathrm{W_{11}}\mathbf{Q}_1 + \mathrm{W_{12}}\mathbf{Q}_2){:}\left(\mathbf{u}_1\mathbf{u}_1 - \frac{\mathbf{I}}{3}\right)$$
$$\Phi_2 = \frac{\partial \mathrm{E_{mix}}}{\partial \mathbf{Q}_2}{:}\left(\mathbf{u}_2\mathbf{u}_2 - \frac{\mathbf{I}}{3}\right) = -\frac{3}{2}(\mathrm{W_{22}}\mathbf{Q}_2 + \mathrm{W_{12}}\mathbf{Q}_1){:}\left(\mathbf{u}_2\mathbf{u}_2 - \frac{\mathbf{I}}{3}\right). \tag{6}$$

The Helmholtz free energy per unit mole of the homogeneous mixture $A(\mathbf{Q}_1, \mathbf{Q}_2)$ is:

$$A(\mathbf{Q}_1, \mathbf{Q}_2) = -N_{\mathrm{A}}(\mathrm{E_{mix}} + k_{\mathrm{B}}\,\mathrm{T} \ln Z) \tag{7}$$

where N_{A} is Avogadros number and the mixture partition function Z is factorised:

$$\mathrm{Z} = Z_1^{\mathrm{m_1}} Z_2^{\mathrm{m_2}} = \left(\int \mathrm{e}^{-\Phi_1/\mathrm{m_1 k_B T}} \mathrm{d}\mathbf{u}_1\right)^{\mathrm{m_1}} \left(\int \mathrm{e}^{-\Phi_2/\mathrm{m_2 k_B T}} \mathrm{d}\mathbf{u}_2\right)^{\mathrm{m_2}} \tag{8}$$

where Z_i is the partition function of the ith species. Equations (5), (7) and (8) are consistent with the thermodynamics (*26*) since they obey

$$\mathrm{E_{mix}} = \frac{\mathrm{d}\beta \mathrm{A}/N_{\mathrm{A}}}{\mathrm{d}\beta} = -\mathrm{E_{mix}} - \frac{\mathrm{d}\ln Z}{\mathrm{d}\beta}. \tag{9}$$

The ten equations of equilibrium are obtained by minimising the free energy A (Equation (7)) with respect to $(\mathbf{Q}_1, \mathbf{Q}_2)$. According to the discussion regarding Equation (3), the binary mixture displays an isotropic state and uniaxial nematic states. Hence, we can safely reduce the solution space (from ten equations to two equations) and parametric space as follows. Scaling the Helmholtz free energy A with the bare interaction parameter $\bar{\mathrm{U}}_{11}$, minimising the resulting dimensionless free energy with respect to $\mathbf{Q}_1$, $\mathbf{Q}_2$, and double-contracting the tensorial equations with $\mathbf{n}_1\mathbf{n}_1$ and $\mathbf{n}_2\mathbf{n}_2$, respectively, we find

$$m_1\varphi_1 S_1 + \frac{3}{2}\sqrt{m_1 m_2 \varphi_1 \varphi_2}\,\wp_1 S_2\left(\cos^2(\alpha) - \frac{1}{3}\right) - T_r \sum_{i=1}^{2} \frac{m_i}{Z_i}\frac{\partial Z_i}{\partial S_1} = 0$$
$$\frac{3}{2}\sqrt{m_1 m_2 \varphi_1 \varphi_2}\,\wp_1 S_1\left(\cos^2(\alpha) - \frac{1}{3}\right) + m_2\varphi_2\wp_2 S_2 - T_r \sum_{i=1}^{2} \frac{m_i}{Z_i}\frac{\partial Z_i}{\partial S_2} = 0 \tag{10}$$

where the partition functions Z_i are defined in Equations (6) and (8). The asymptotic limits of Equations (10) (m_1=0,1) of this expression correspond to the pure nematic LC. As shown below for the present CM case, the mixture is uniaxial and α=0. The thermodynamic of the mixture is defined by the dimensionless temperature T_r and two effective molar fractions:

$$T_r = \frac{k_B T}{\bar{U}_{11}};\quad \varphi_i = \frac{m_i M w_i}{\sum m_i M w_i}. \tag{11}$$

The two material parameters of the model are

$$\wp_1 = \frac{\bar{U}_{12}}{\bar{U}_{11}};\quad \wp_2 = \frac{\bar{U}_{22}}{\bar{U}_{11}}. \tag{12}$$

The material parameters $(\wp_1, \wp_2)$ are functions of the species' molecular weights. To introduce the molecular weight dependence we use experimental data (*19*) in conjunction with the well-known relation $\bar{\mathrm{U}}_{\mathrm{ii}} = 4.542\mathrm{kT_{NIi}}$, where the clearing temperature $T_{\mathrm{NI}i}$ is a function of the molecular weight $M_{\mathrm{w}i}$. Experimental data on CMs suggest that this dependence is well fitted by a linear function

$$\mathrm{T_{NIi}} = \bar{\mathrm{U}}_{\mathrm{ii}}/4.542\mathrm{k} = a + b\ \mathrm{Mw_i} \tag{13}$$

where the parameters a, b, based on the data of (*24*), are chosen as $a = -150$ and $b = 0.75$.

We choose component '1' as a representative component of a CM with $M_{\mathrm{w1}} = 1400$ (see (*10*)) and

vary the molecular weight M_{w2} of the second component so that molecular weight asymmetry $\Delta M_w = M_{w1} - M_{w2}$ changes. Using Equations (12), (13) and experimental data we find the following molecular weight dependence of $\wp_2$:

$$\wp_2 = \frac{\bar{U}_{22}}{\bar{U}_{11}} = \frac{4.542kT_{NI2}(Mw_2)}{4.542kT_{NI1}(Mw_1)} = \frac{c + d\,Mw_2}{c + d\,Mw_1} \qquad (14)$$

where c, d are constants. Since the molecular weight dependence of $\wp_1$ is not suggested by actual data, we use

$$\wp_1 = \beta\wp_2 \qquad (15)$$

where β is a constant whose sign depends on the geometrical nature of the species: for the similar components, i.e. disks and disks or rods and rods, it is positive; however, for dissimilar components it is negative (*27*). We note that taking β as another material parameter will not affect the essential nature of the results (i.e. the presence of the ordering states (I, N)) but will only shift phase transition curves in the thermodynamic phase diagram.

The present thermodynamic model is given by the two non-linear integral equations (Equations (10)); the solution vector consists of the two scalar order parameters (s_1, s_2); the two material parameters are β and ΔM_w; the thermodynamic phase diagram is obtained by sweeping over temperature T_r and concentration m_1. Equations (10) are solved by Newton–Raphson method, with an eighth-order Simpson integration method. Stability, accuracy and convergence were ensured using standard methods. For the higher values of the molecular weight asymmetry and the higher values of the interaction parameter, the numerical algorithm exhibits multiple solutions in the vicinity of the transition temperature. Depending on the values of the initial guess, the final solution vector would be different. Therefore, the values of the free energy are compared for different initial guesses and that with the minimum energy is selected as the correct solution. Issues of metastability are not considered in this paper.

3. Characterisation methods

3.1 Computation of the interaction parameter for critical mixtures

In this section, we present tools to characterise non-ideal mixtures that exhibit a minimum in the NI transition temperature corresponding to a concentration at which the two species form a pseudo-pure component nematic. Different experimental studies have reported a pronounced minimum in the transition temperature of the liquid crystalline mixtures as a function of the concentration (*8, 28–30*). However, theses studies have not addressed the effect of intrinsic parameters involved in the CM mixtures, the most important one being the molecular weight asymmetry. The minimum in the phase diagram (see Figure 1(c)) shows a weak interaction between the components. To calculate the values of the interaction parameter, β, of a given nematogen mixture with specific critical concentration and molecular weight asymmetry, we solve Equations (10) with $s_1 = s_2$ and obtain

$$\beta = \frac{(1 - m_{1c})\left(1 - \frac{\Delta Mw}{Mw_1}\right)\left(\frac{T_{rNI2}}{T_{rNI1}}\right) - m_{1c}}{(1 - 2m_{1c})\sqrt{\left(1 - \frac{\Delta Mw}{Mw_1}\right)\left(\frac{T_{rNI2}}{T_{rNI1}}\right)}}. \qquad (16)$$

Once we determine the value of the critical concentration (m_{1c}) for a mixture with known molecular weights (M_{w1}, M_{w2}) and transition temperatures (T_{rNI1}, T_{rNI2}), the interaction parameter β can be calculated by using Equation (16). In Section 4.3, we show how to determine the critical concentration and how to find the interaction parameter by using Equation (16).

3.2 X-Ray intensity

The solution vector (s_1, s_2) to Equations (10) is used to predict X-ray intensity using previously derived equations (*26*). The X-ray intensity $I_i(\theta)$ of a single-component nematic LC, when assumed to follow the MS theory, is (*31*)

$$I_i(\theta) = \frac{\sqrt{\pi}}{2} ODF_i(\theta) \frac{\mathrm{erf}\left(\sqrt{-\phi_i(\theta)/m_i kT}\right)}{\sqrt{-\phi_i(\theta)/m_i kT}} \qquad (17)$$

where the single species orientation distribution function is

$$ODF_i = \exp(-\phi_i/m_i kT)/Z_i \qquad (18)$$

and erf is the error function. Measuring $I_i(\theta)$ is thus a useful way to determine the orientation distribution function $ODF_1(\theta)$. A review of application of Equation (17) in conjunction with the MS theory is given in (*32*). For a uniaxial nematic mixture ($\alpha = 0$; see Figure 2) we can safely assume that Equation (17) holds. Using this assumption we find the mixture X-ray intensity $I_{mix}(\theta)$:

$$I_{mix}(\theta) = \frac{\sqrt{\pi}}{2} ODF_{mix} \frac{\mathrm{erf}\left(\sqrt{-\phi_{mix}(\theta)/kT}\right)}{\sqrt{-\phi_{mix}(\theta)/kT}} \qquad (19)$$

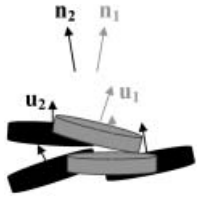

Figure 3. Schematic of a binary mixture of discotic nematogens, representative of a carbonaceous mesophase mixture.

where the mixture orientation function $\mathrm{ODF_{mix}}$ and the mixture MS mean field potential ϕ_{mix} are (see Appendix 2)

$$\begin{aligned}\mathrm{ODF_{mix}} &= m_1\mathrm{ODF}_1 + m_2\mathrm{ODF}_2 \\ &= \exp(-\phi_{\mathrm{mix}}(\theta)/\mathrm{kT})/\mathrm{Z_{mix}} \\ -\phi_{\mathrm{mix}}(\theta)/\mathrm{kT} &= \ln(\mathrm{Z_{mix}}(m_1\mathrm{ODF}_1 + m_2\mathrm{ODF}_2)).\end{aligned} \tag{20}$$

In this work, we solve Equations (10) for selected

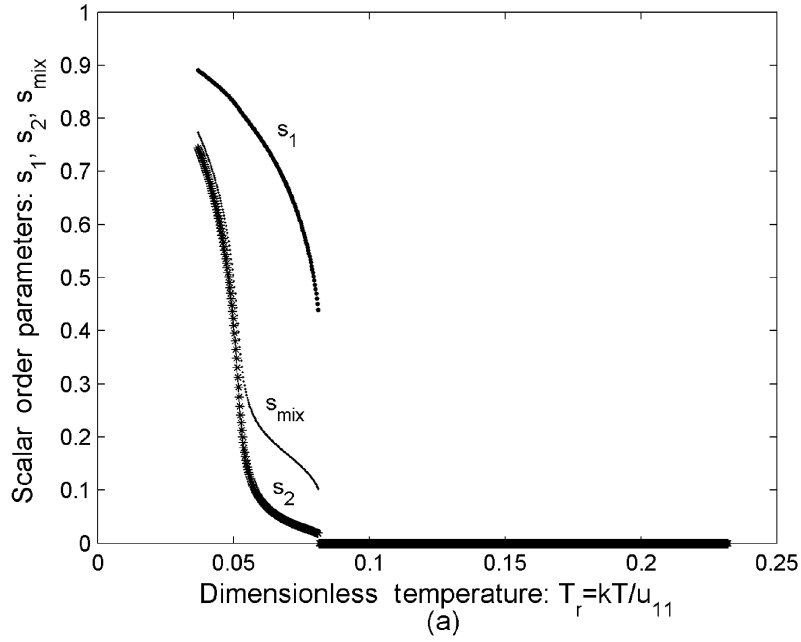

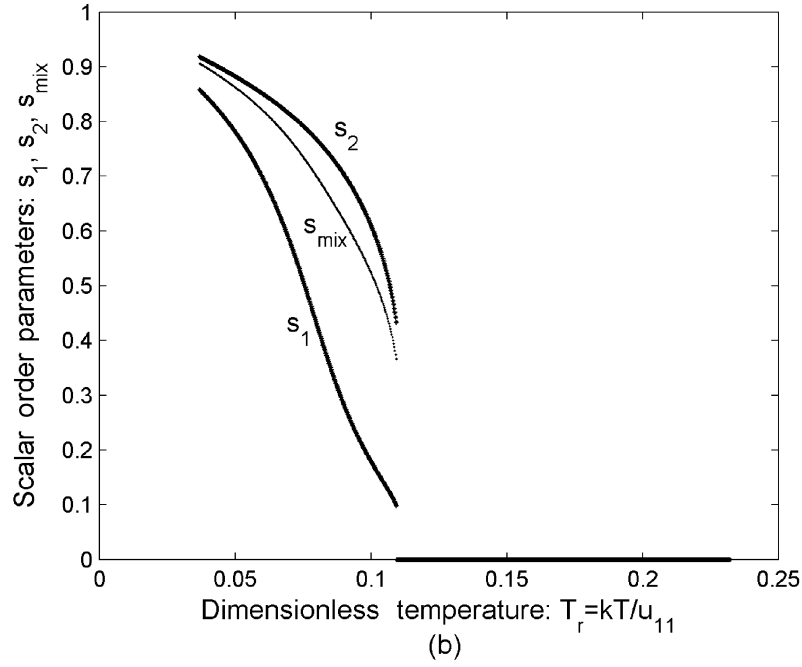

Figure 4. Scalar order parameters (s_1, s_2 and s_{mix}) as a function of reduced temperature for m_1=0.2 and β=0.1, for (a) ΔM_{w}=800 (M_{w2}=600) and (b) ΔM_{w}=400 (M_{w2}=1000).

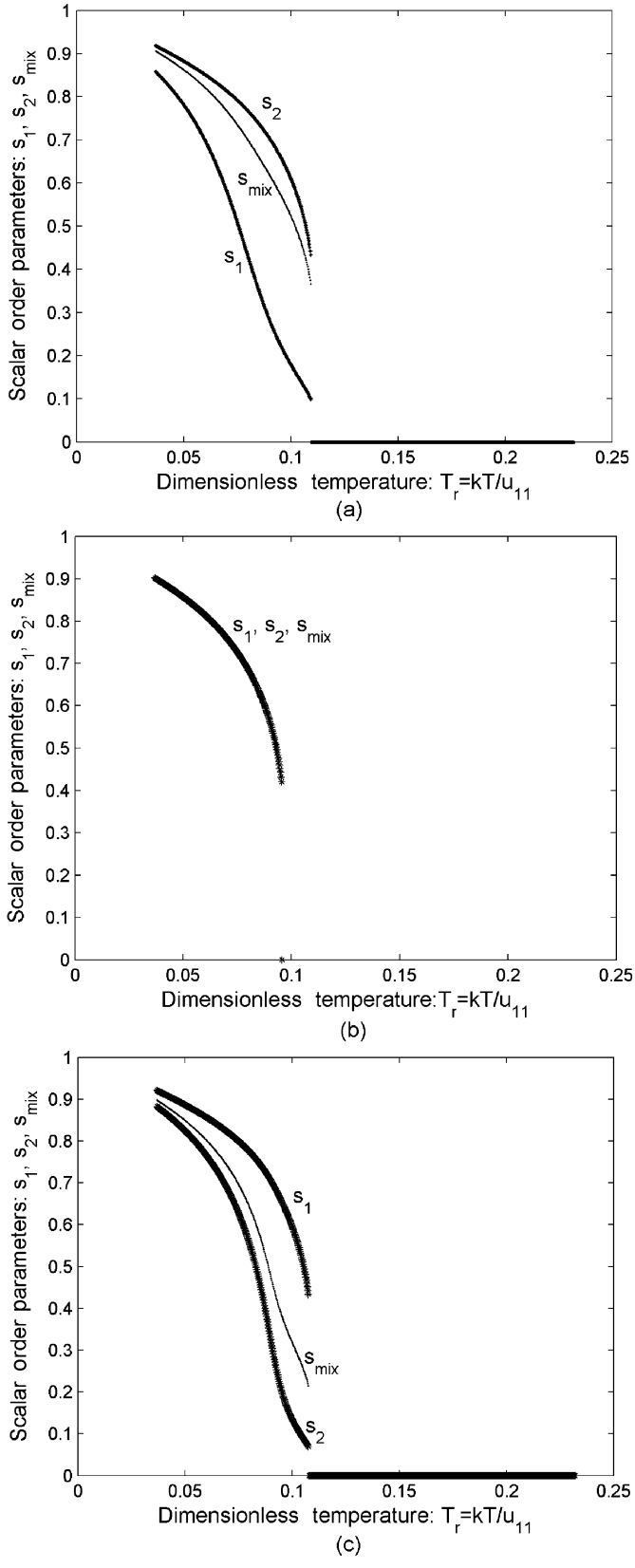

Figure 5. Scalar order parameters (s_1, s_2 and s_{mix}) as a function of dimensionless temperature, for $\beta=0.1$ and $\Delta M_w=1000$ for: (a) $m_1=0.2$; (b) $m_1=0.31$; (c) $m_1=0.4$.

areas of the (T_r, m_1) phase diagram, calculate the ODF using Equations (18) and (20), and then use the results in conjunction with Equation (19) to compute $I_{\mathrm{mix}}(\theta)$.

4. Results and discussion

4.1. Structure of the nematic phase

4.1.1. Relative alignment (α).

The relative alignment α defines the nature of the nematic mixture: (i) uniaxial, $\alpha=0$ and (ii) biaxial, $\alpha\neq0$. In the original tensorial formulation, minimising A (Equation (7)) with respect to ($\mathbf{Q}_1$, $\mathbf{Q}_2$) determines α. For mixtures of uniaxial discs differing only in molecular weight, α is zero and the nematic mixture is therefore uniaxial (Figures 2 and 3). Under external fields such as confinement, flow, magnetic and electrical fields, α is an unknown (*33–35*).

4.1.2. Effect of molecular weight difference.

This section shows how the state (I, N) and the phase transition of the binary mixture depends on the molecular weight difference $\Delta M_{\mathrm{w}}=1400-M_{\mathrm{w}2}$.

Figure 4 shows the scalar order parameters s_1, s_2 and s_{mix} as functions of the dimensionless temperature T_r, for $m_1=0.2$, $\beta=0.1$, $\Delta M_{\mathrm{w}}=800$ (Figure 4(a)) and 400 (Figure 4(b)). At sufficiently high ΔM_{w} (Figure 4(a)), the lower molecular weight component has less ordering in spite of its higher concentration. At high enough temperatures a concavity is observed in its ordering trend. It emerges from the intrinsic tendency of the component with the lower molecular weight to be isotropic; however, due to the interaction (β) it is energetically preferable to be in the nematic state. The first-order NI phase transition takes place at $T_r=0.095$. At lower ΔM_{w} (Figure 4(b)) the low melting component controls the ordering of the mixture due to its dominant concentration and the NI transition takes place at $T_r=0.109$.

4.1.3. Dilution effect (m_1).

Mesogenic mixtures exhibit both lyotropic and thermotropic behaviour, $s_i(T, m_1)$, and dilution (changes in m_1) drives the phase transition, as in other lyotropic LCs (*36*).

Figure 5 shows the scalar order parameters s_1 and s_2 as a function of dimensionless temperature T_r, for $\beta=0.1$, $\Delta M_{\mathrm{w}}=400$, $m_1=0.2$ (Figure 5(a)), 0.31 (Figure 5(b)) and 0.4 (Figure 5(c)). In this case the minority component '1' has the higher molecular weight and higher T_{NI} value, but dilution introduces the lyotropic effect. At high dilution (Figure 5(a)) as T_r increases the minority component has more tendency to convert to the isotropic phase. Transition takes place at $T_r=0.109$. As the concentration increases (Figure 5(b)) both the minority and the majority components exhibit a similar ordering and the mixture behaves like a pure system. The transition takes place at $T_r=0.095$ which shows a decrease compared with $m_1=0.2$. We use the term 'critical

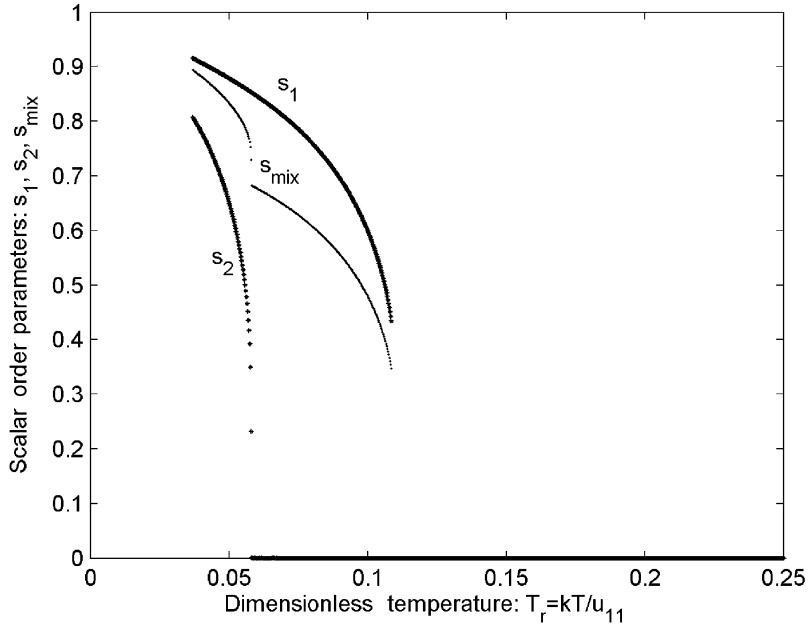

Figure 6. Scalar order parameters (s_1, s_2 and s_{mix}) as a function of dimensionless temperature, for $m_1=0.2$ and $\Delta M_{\mathrm{w}}=400$ and $\beta=0$ (no interaction).

mixture' for this system and 'critical concentration' for the corresponding concentration (0.31 here). At $m_1=0.4$ (Figure 5(c)) the majority component has less ordering due to its lower M_w and tends to be in the isotropic state; in this case transition takes place at $T_r=0.108$.

In partial summary, binary mixtures exhibit both lyotropic and thermotropic behaviour. A minority component of relatively high M_w at low temperatures may nevertheless exhibit low ordering due to the lyotropic effect.

4.1.4. *Effect of the interaction parameter (β).*

In the absence of interactions, β=0, the mixture is ideal and the two mesogens are unaffected by each other and each undergoes the clearing transition independently. Figure 6 shows scalar order

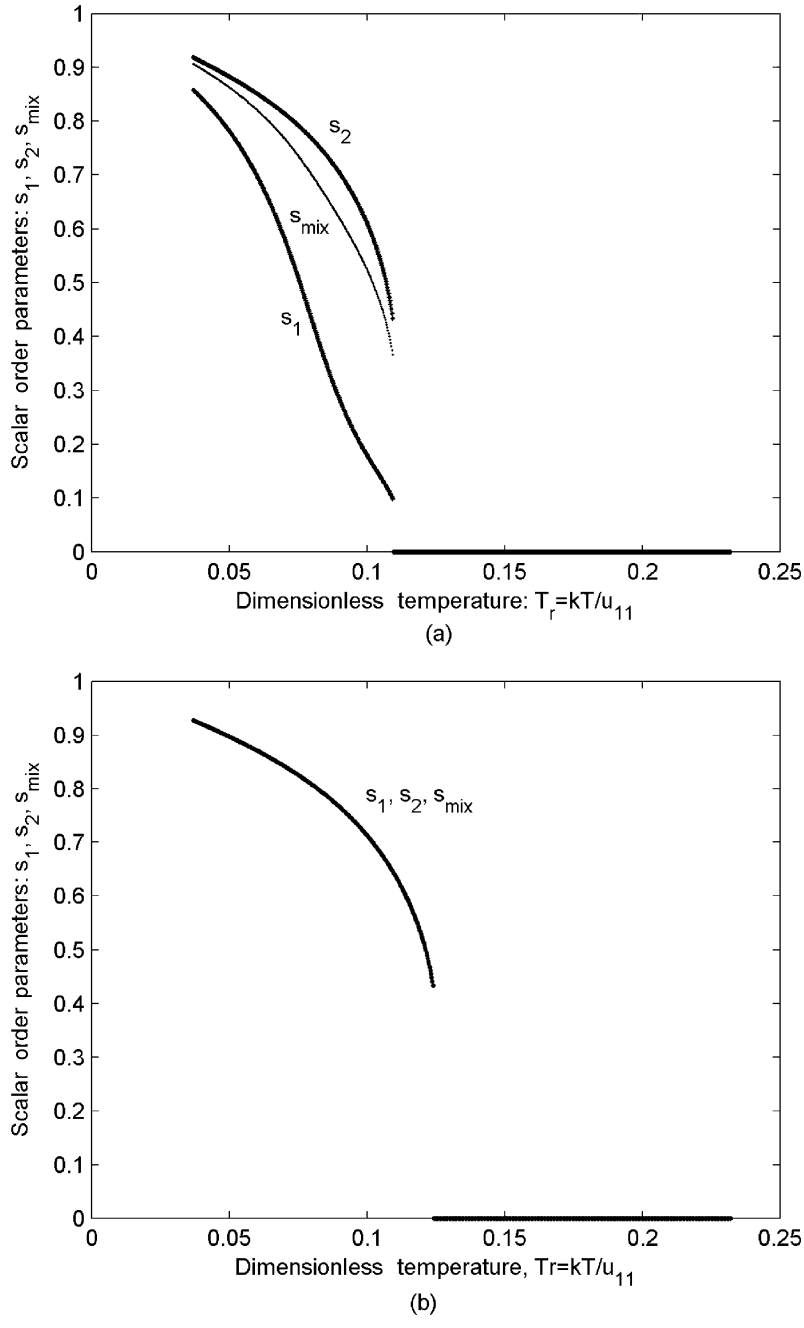

Figure 7. Scalar order parameters (s_1, s_2 and s_{mix}) as a function of dimensionless temperature, for $m_1=0.2$, and $\Delta M_w=400$ for two different interaction parameters: (a) β=0.1 and (b) β=0.5. For highly interacting mixtures the contribution of the higher molecular weight component '1' to the ordering becomes enhanced so that $s_1=s_2$, although $m_1 \ll m_2$.

parameters s_1, s_2 and s_{mix} as functions of the dimensionless temperature T_r for $\Delta M_w=400$, $m_1=0.2$ and $\beta=0$. However, when $\beta\neq 0$ there is a single mixture clearing temperature. Figure 7 shows the scalar order parameters s_1, s_2 and s_{mix} as functions of the dimensionless temperature T_r for $\Delta M_w=400$, $m_1=0.2$, $\beta=0.1$ (Figure 7(a)) and 0.5 (Figure 7(b)). The figure shows that for this weakly asymmetric mixture ($\Delta M_w=400$), weak coupling (Figure 7(a)) leads to coexisting nematic phases with different ordering ($s_2>s_1$), but strong coupling (Figure 7(b)) leads to a critical mixture. Hence, increasing the interaction enhances the effect of molecular weight asymmetry.

4.2. Phase diagrams

In this section we use Equation (16) to classify the T–m phase diagrams. Figure 8 shows the classification of the mixtures in terms of molecular weight asymmetry and interaction parameter, showing the property envelopes for ideal and non-ideal mixtures. The coefficients a and b applied in Equation (13) restricts the minimum value of M_{w2} as 200. Therefore, the horizontal dashed line shows the limit of ΔM_w which is physically meaningful within the model (1400−200=1200). The solid curve that separates ideal from non-ideal behaviour is a plot of Equation (16) with $m_{1c}=0$. The other distinguishing features of Figure 8 are: (i) for equal molecular weight, non-ideality arises only under weaker interaction; (ii) as the M_w asymmetry increases, ideal behaviour arises with weaker interaction.

Figure 9 shows the phase diagram of two mixtures, representing the two regions A and B in Figure 8. (i) The mixture in region A behaves non-ideally and exhibits a minimum in its phase diagram; the mixture with the minimum transition temperature T_{NI} is the critical mixture where $s_1=s_2$ (Figure 9(a)). (ii) The mixture in region B, which has large molecular weight asymmetry and large interaction parameter, behaves ideally and shows a monotonic increase in the transition temperature T_{NI} as a function of the concentration (Figure 9(b)); as a result, a critical mixture cannot be obtained from this region.

Figure 10 shows the critical concentration as a function of ΔM_w and β, using Equation (16). As the interaction β increases the concentration needed to obtain the critical mixture with a specific ΔM_w decreases. In other words, the larger value of β enhances the effect of the component with higher molecular weight. Therefore, it controls the overall order parameter of the mixture, even at a lower concentration, in contrast to the system with a smaller β. All of the graphs reach the zero critical concentration. In the case of the zero critical concentration the critical mixture forms at $m_1=0$. In other words the first component (with the higher molecular weight) always controls the overall

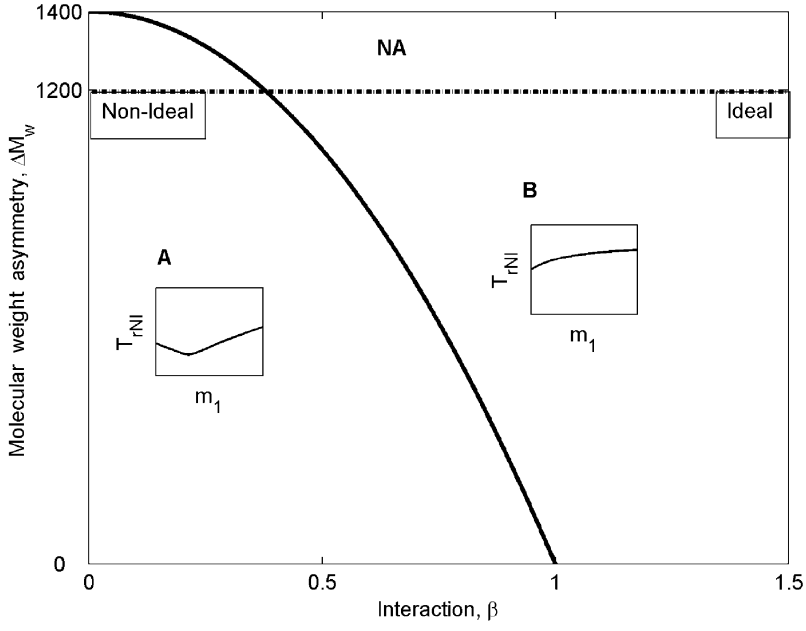

Figure 8. Classification of the mixtures into two types, type A with the non-ideal behaviour and type B with ideal behaviour, based on their intrinsic properties: M_w asymmetry ΔM_w and the interaction parameter β. For weakly interacting mixtures and/or small molecular weight asymmetry the nematic–isotropic (NI) transition line exhibits a minimum by increasing the concentration (region A); however, for sufficiently strongly interacting mixtures and/or sufficiently large molecular weight asymmetry the NI transition line is monotonic (region B).

orientation of the mixture. In the other words, s_1 is always greater than s_2. The second component can control the overall orientation, only when $m_1=0$.

Figures 11 shows the effect of β on the temperature-composition thermodynamic phase diagram for $\Delta M_w=400$ and β=0 (no interaction) (Figure 11(a)); β=0.1, 0.2 and 0.5 (Figure 11(b)); I_i denotes isotropic and N_i denotes nematic. Under no interaction (Figure 11(a)) there are two clearing transition lines and in the region below the transition lines, coexisting nematic and nematic–isotropic phases are observed. As the interaction increases (β ↑) the crossing transition lines merge (Figure 11(b)) to define the mixture isotropic–nematic transition line. The nematic region contains two parts: N_{21} with $s_2>s_1$ for the left part and N_{12} with $s_1>s_2$ for the right part. The boundary between these two regions corresponds to the critical concentration which makes the critical mixture, where $s_1=s_2$ and where the transition temperature has the minimum. By increasing the interaction

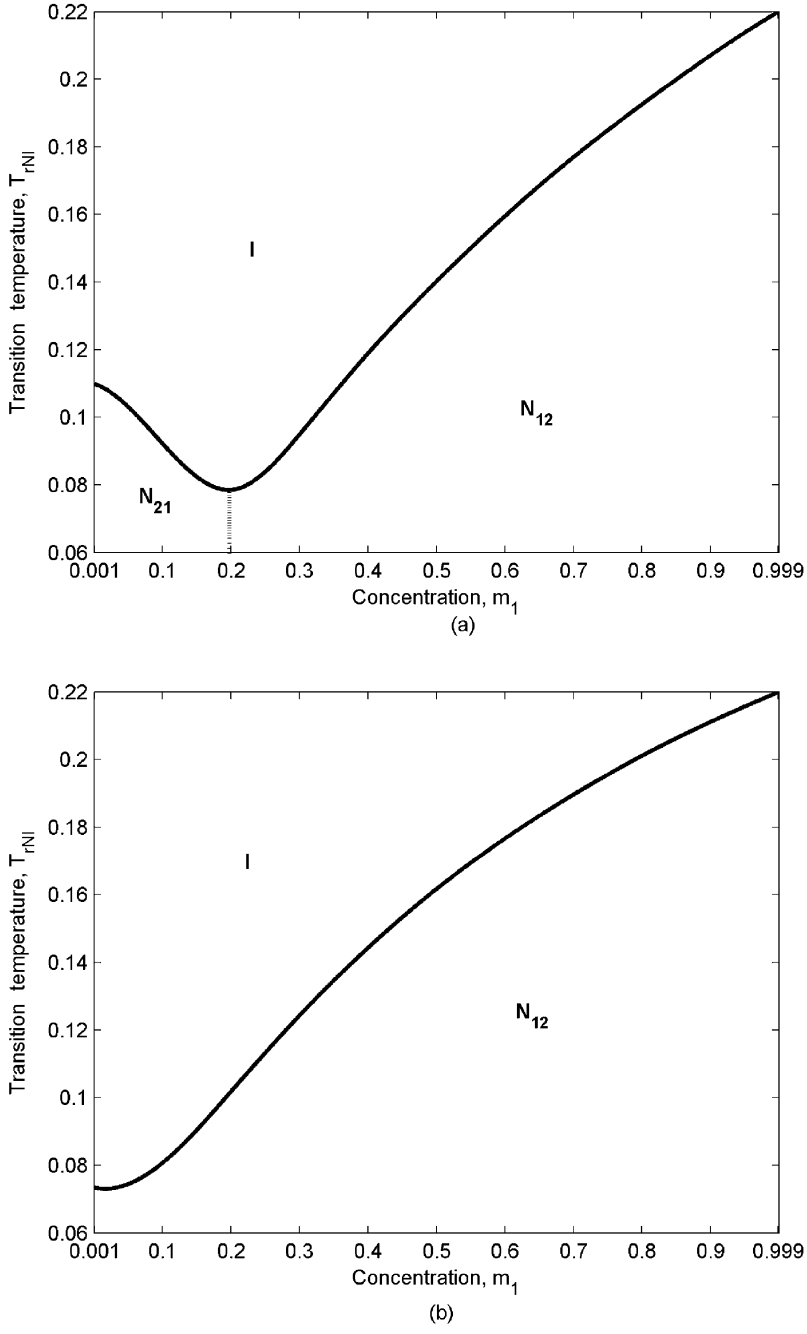

Figure 9. Temperature-composition thermodynamic phase diagram for two different types of mixtures: (a) non-ideal (with $\Delta M_w=600$ and β=0.1); and (b) ideal (with $\Delta M_w=800$ and β=1).

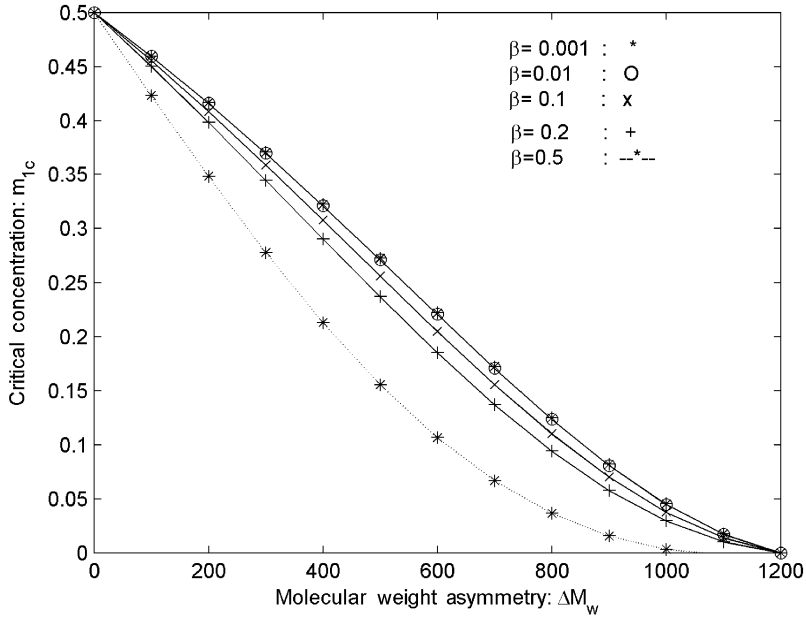

Figure 10. Critical concentration as a function of the intrinsic properties: molecular weight asymmetry and the interaction parameter.

parameter, β, the tendency of the component with the lower M_w to remain nematic increases; as a result, transition to the isotropic phase shifts to higher temperatures.

4.3 Critical concentration detection

As mentioned above, the orderings of CM mixtures are affected by the lyotropic and thermotropic effects. Concentration can shift the phase transition and any related phenomena of the mixture along the temperature axis. For instance, the final structure of the CM-based fibres which is dictated by the temperature effect (*21*) is influenced by concentration values. Therefore, it is of key importance to determine whether a specific mixture can produce a non-ideal behaviour and if it can reach a minimum transition temperature. It is also crucial to detect the critical concentration of the mixture, if it exists. In the following section, we propose predictive tools to detect the critical concentration.

4.3.1 X-ray intensity.

Here we present the X-ray intensity I_{mix} calculations of the mixture using Equations (19) and (20). Figure 12 shows the values of the intensity parallel to the director $\theta=0$ (maximum intensity) as a function of concentration m_1, at a constant temperature $T=320$ K for $\beta=0.1$ and molecular weight asymmetry $\Delta M_w=400$ (Figure 12(a)) and $\beta=1$ and molecular weight asymmetry $\Delta M_w=800$ (Figure 12(b)). The intrinsic properties for Figure 12(a) correspond to the non-deal region in Figure 8. The minimum value of the intensity corresponds to the most uniform distribution function which represents the least ordered state. This phenomenon takes place in the vicinity of the critical concentration. Therefore, we can significantly decrease the range of the concentration in which the critical concentration exists. Figure 12(b) show the corresponding predictions for an ideal mixture and agrees with the expectation of a monotonic increase. Therefore, by using X-ray intensity we can: (i) determine the mixture type and hence whether a critical concentration exists or not; (ii) estimate a range of the concentration (for non-ideal mixtures) in which the critical concentration exists. This narrowed concentration range can then be used more effectively to determine the exact value of the critical concentration, using direct methods that we mention next.

4.3.2 Direct Methods.

Here we discuss methods that can be used to determine the critical concentration based on direct measurements of the scalar order parameter.

Figure 13 shows the average ordering, s_{mix}, at the transition $s_{mix}|_{TNI}$, as the ordering criterion, as a function of concentration for two types of behaviour corresponding to Figure 12. Figure 13(a) depicts the typical ordering trend of the mixture which behaves non-ideally. Two local minima and a local maximum are observed here. There are three regions in this

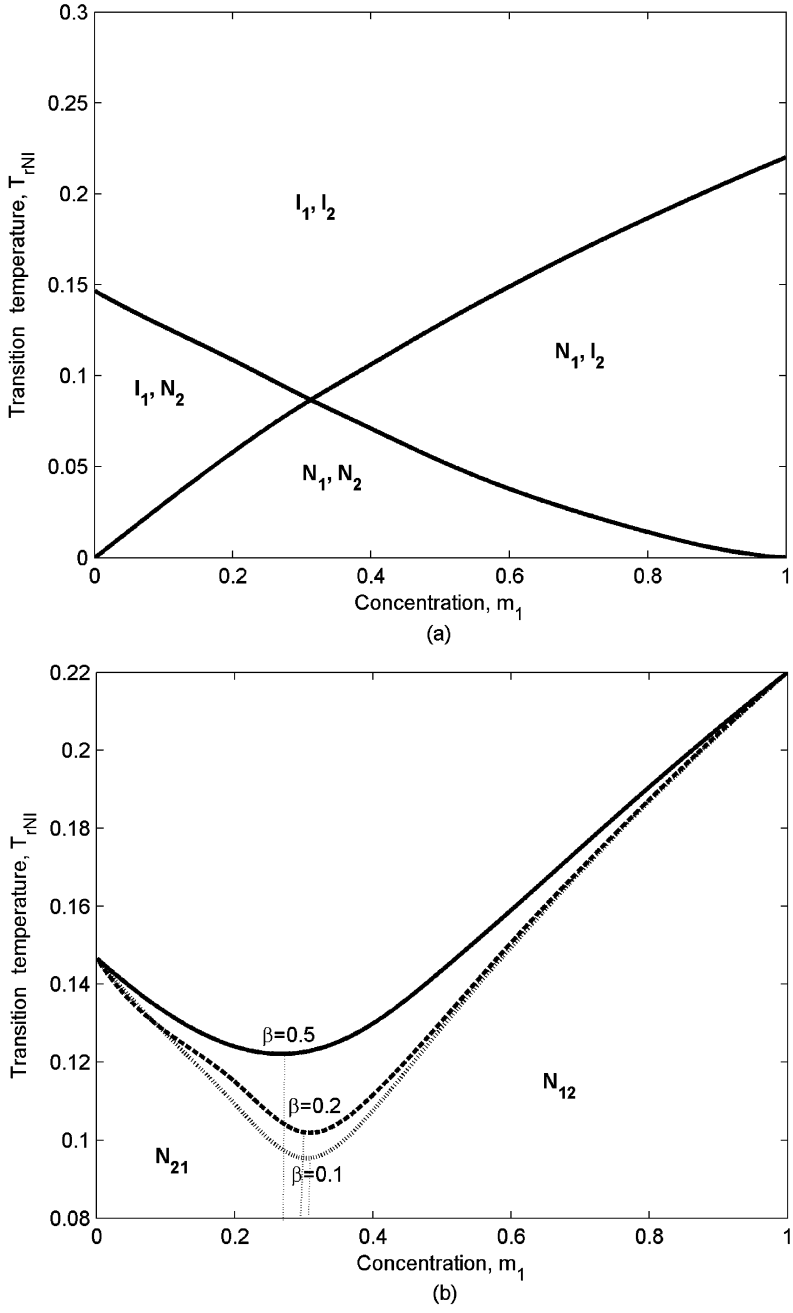

Figure 11. Temperature-composition thermodynamic phase diagram for ΔM_w=400 and: (a) β=0 (no interaction); (b) β=0.1, 0.2 and 0.5. Two transition lines in the non-interaction case (a) converts to angle nematic to isotropic transition line for the interacting cases (b). Strong interaction results in the higher nematic–isotropic transition temperature.

graph: (i) below m_{1c}, $s_2 \gg s_1$ (which corresponds to N_{21}); in this section s_{mix} decreases by increasing concentration (as s_2 decreases); (ii) above m_{1c}, $s_1 \gg s_2$ (which corresponds to N_{12}): in this section s_1 and s_{mix} increase as concentration increases; (iii) in the vicinity of m_{1c}, $s_1 \approx s_2$ (which corresponds to the transition region); in this section the controlling component is changing and as a result, a maximum which takes place at the critical concentration appears in the graph. However, for the ideal case (Figure 13(b)), a single minimum is observed. This figure shows the typical ordering trend of the mixture which behaves ideally. In this case the maximum corresponding to the non-ideal trend moves to lower concentrations and then disappears, resulting in an ideal behaviour. There is no critical concentration in this case and the component with higher molecular weight always controls the overall ordering. Therefore, experimental

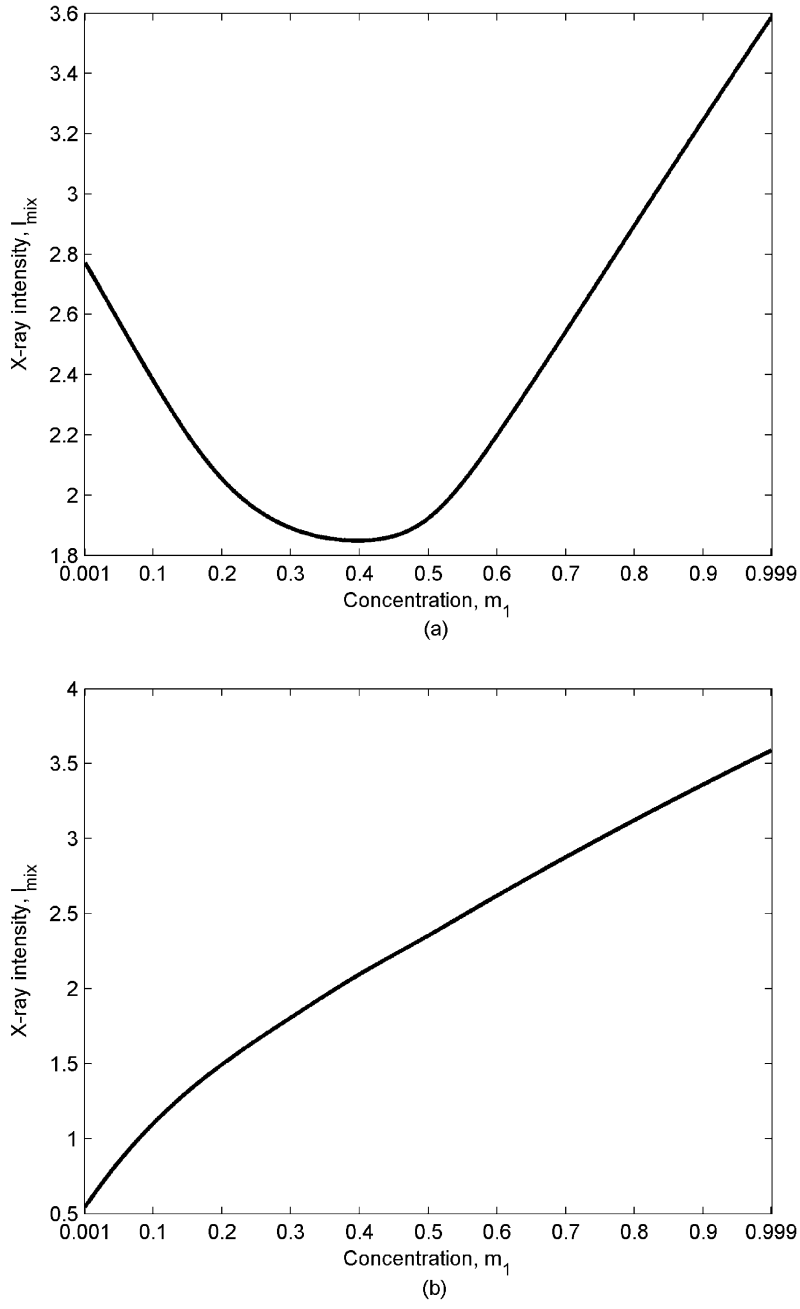

Figure 12. The maximum value of the X-ray intensity as a function of the concentration at $T=320\,\mathrm{K}$ for: (a) $\Delta M_w=400$, $\beta=0.1$ (non-ideal); and (b) $\Delta M_w=800$, $\beta=1$ (ideal).

methods such as nuclear magnetic resonance (NMR) spectroscopy, diamagnetic anisotropy and refractive indices which measure scalar order parameters of the mixture and its individual components (*19, 27, 37, 38*) can be used to detect the type of the mixture as well as the value of the critical concentration.

5. Conclusions

In this paper we have extended the MS model to binary mixtures of discotic nematogens. The thermotropic and lyotropic behaviour of the mixtures are demonstrated by phase transitions induced by temperature and concentration changes. Based on the molecular weight asymmetry and the interaction parameter, mixtures are classified as ideal and non-ideal. Each type exhibits a distinguished temperature-concentration phase behaviour, as well as a specific ordering trend. (i) Non-ideal mixtures with non-monotonic NI transition temperatures and reversal of ordering $\left(s_1 > s_2 \rightleftarrows s_2 > s_1\right)$ due to the concentration effect; the value of the concentration at which this

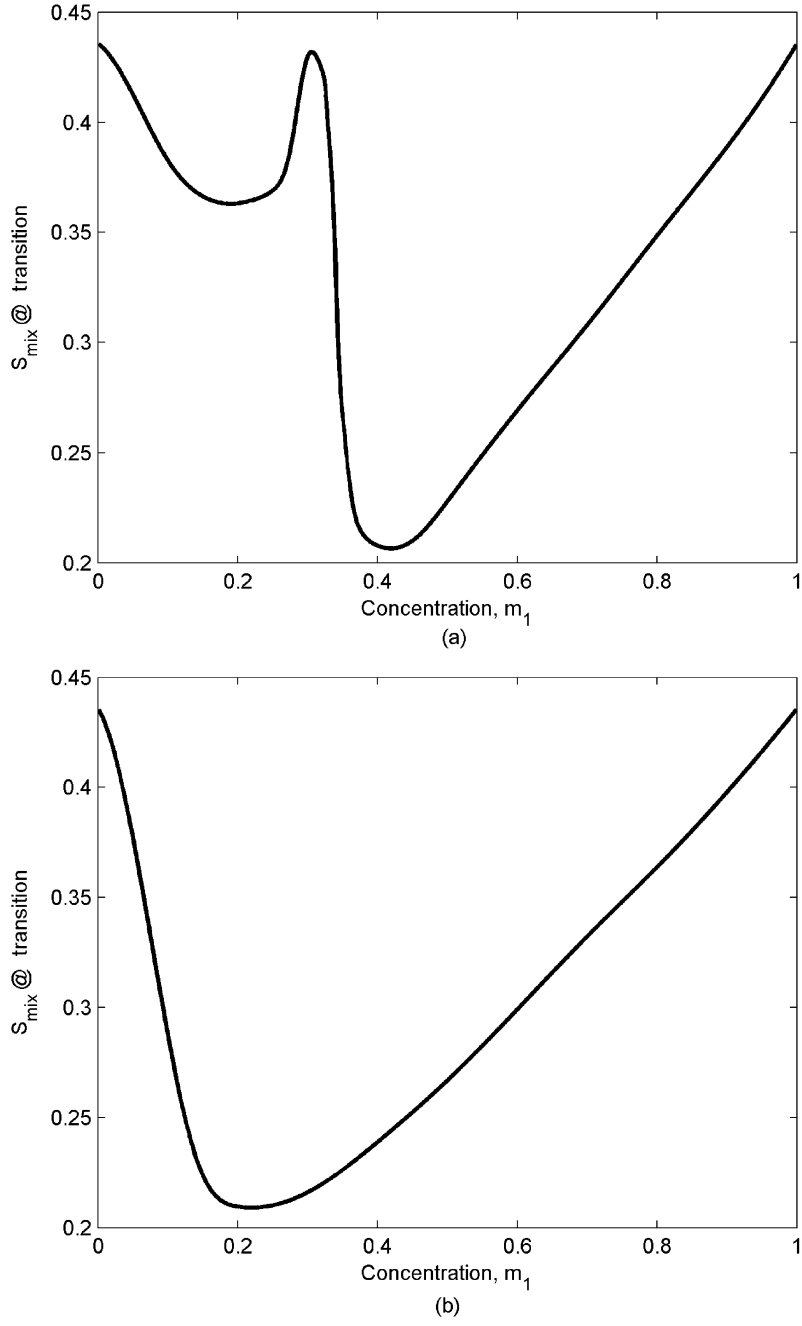

Figure 13. Scalar order parameter of the mixture at the transition temperature $s_{mix}|_{TNI}$ as a function of concentration for: (a) ΔM_w=400, β=0.1(non-ideal); and (b) ΔM_w=800, β=1 (ideal). Maximum ordering at the transition is observed at the critical concentration for the non-ideal type. No maximum is observed for the ideal case.

transition takes place is the critical concentration. The mixture exhibits the minimum value of the transition temperature at the critical concentration. The average ordering of this type of mixtures, at the NI transition, shows two minima and a local maximum corresponding to the critical concentration; this case is obtained for weakly interacting mixtures and its phase diagram shows lyotropic/thermotropic behaviour. (ii) Ideal mixtures correspond to the sufficiently strong interaction and highly asymmetric molecular weights; for this case the NI transition temperature monotonically changes by increasing the concentration. The mixture behaves ideally and a critical concentration with ordering reversal cannot be obtained. Its average ordering at the NI transition also changes monotonically with concentration. The mixture type as well as the value of the critical concentration can be determined by X-ray intensity

measurements. They also can be detected by any experimental method which measures scalar order parameters.

In summary, the MS mixture model is a predictive tool that can be used to assess the nematic ordering of the mixture in response to the combined lyotropic and thermotropic effects and to control the NI transition using molecular weight asymmetry and molecular interaction as parameters.

Acknowledgements

Support was provided by the National Science Foundation under Award Number EEC-9731689 and the Petroleum Research Fund of the American Chemical Society.

References

(1) Singer L.S. *Faraday Discuss.* **1985**, *79*, 265–272.
(2) Sheikh S.Y. The effect of composition and shear rate on mesophase mixtures, *MS Thesis*, Clemson University, Clemson, SC, 1999.
(3) Marsh H. *Fuel* **1973**, *52*, 205–212.
(4) Gupta G.; Rey A.D. *Phys. Rev. Lett.* **2005**, *95*, 127802:1–127802:4.
(5) Edie D.D.; Robinson K.E.; Fleurot O.; Jones S.P.; Fain C.C. *Carbon* **1994**, *32*, 1045–1054.
(6) Hurt R.H.; Hu Y. *Carbon* **1999**, *37*, 281–292.
(7) Yoon S.H.; Korai Y.; Mochida I. *Carbon* **1993**, *31*, 849–856.
(8) Naggapa S.; Nataraju S.K.; Marthandappa M. *Mol. Cryst. Liq. Cryst.* **1991**, *197*, 15–20.
(9) Yan J.; Rey A.D. *Phys. Rev. E* **2002**, *65*, 031713:1–031713:14.
(10) Cervo E.G.; Thies M.C. *Chem. Eng. Technol.* **2007**, *30*, 742–748.
(11) Brochard F.; Jouffroy J.; Levinson P. *J. Physique* **1984**, *45*, 1125.
(12) Humphrieps R.L.; James G.; Luckhurst G.R. *Symp. Faraday Soc.* **1971**, *5*, 107–118.
(13) Bates G.S.; Beckmann P.A.; Burnell E.E. *Mol. Phys.* **1986**, *57*, 351–357.
(14) Muhoray P.P.; Dunmur D.A.; Miller W.H. *Liq. Cryst. Ordered Fluids* **1984**, *4*, 615–641.
(15) Beauharnois M.E.; Edie D.D.; Thies M.C. *Carbon* **2001**, *39*, 2101–2111.
(16) Yang D.K.; Yin Y.; Liu H. *Liq. Cryst* **2007**, *34*, 605–609.
(17) Barbero G.; Evangelista L.R. *Phys. Rev. E* **2000**, *61*, 2749–2752.
(18) Stephen M.J.; Straley J.P. *Rev. Mod. Phys.* **1974**, *46*, 617–702.
(19) Chandrasekhar S. *Liquid Crystals*, 2nd edn; Cambridge University Press: New York, 1992.
(20) Muhoray P.P.; de Bruyn J.J. *Mol. Cryst. Liq. Cryst.* **1985**, *127*, 301–319.
(21) Yan J.; Rey A.D. *Carbon* **2002**, *40*, 2647–2660.
(22) Rey A.D.; Denn M.M. *Annu. Rev. Fluid Mech.* **2002**, *34*, 233–266.
(23) Zimmer J.E.; White J.L. *Adv. Liq. Cryst.* **1982**, *5*, 157.
(24) Hu Y.; Hurt R.H. *Carbon* **2001**, *39*, 887–896.
(25) L'huillier D.; Rey A.D. *J. Non-Newton. Fluid Mech.* **2004**, *120*, 85–92.
(26) Priestley E.B.; Wojtowicz P.J.; Sheng P. *Introduction to Liquid Crystals*; Plenum Press: New York, 1974.
(27) Bates G.S.; Burnell E.E.; Hoatson G.L.; Muhoray P.P.; Weaver A. *Chem. Phys. Lett.* **1986**, *134*, 161–165.
(28) Naggapa S.; Mahadeva J.; Somashekarappa H.; Somashekar R. *Indian J. Phys. Proc. Indian Assoc. Cultivation Sci. A* **2000**, *74*, 45–48.
(29) Sarkar P.; Sarkar P.K.; Paul S.; Mandal P. *Phase Transitions* **2000**, *71*, 1–12.
(30) Nagappa S.; Jagadish K.N.; Mahadeva J.; Naveenkumar S.K.; Somashekar R. *Mol. Cryst. Liq. Cryst.* **2001**, *366*, 239–246.
(31) Sori M. Calorimetric measurments in nematics. In *Physical Properties of Liquid Crystals: Nematics*; Dunmur D.A., Fukuda A., Luckhurst G.R. (Eds), INSPEC: London, 2001. pp. 14–50.
(32) Davidson P.; Petermann D.; Levelut A.M. *J. Phys. II France* **1995**, *5*, 113–132.
(33) Rey A.D. *Liq. Cryst* **1996**, *20*, 147–159.
(34) Rey A.D. *Rheol. Acta* **1995**, *34*, 461–473.
(35) Rey A.D. *Mol. Cryst. Liq. Cryst.* **1996**, *281*, 155–170.
(36) De Gennes P.G.; Prost J. *The Physics of Liquid crystals*, 2nd edn; Clarendon Press: Oxford, 1995.
(37) Delhaes P.; Rouillon J.C.; Fug G.; Singer L.S. *Carbon* **1979**, *17*, 435–440.
(38) Hsu M.L.; Grant D.M.; Pugmire R.J.; Korai Y.; Yoon S.H.; Mochida I. *Carbon* **1996**, *34*, 729–739.

Appendix I: Maier-Saupe model

In this section, we briefly sketch the MS model for a single-component nematic LCs, which is necessary in developing the binary mixture model. According to the Doi–Maier–Saupe model the internal potential $\Phi(\mathbf{u})$ acting on a molecule of orientation $\mathbf{u}$ in a single-component LC is given by the following expression:

$$\Phi(\mathbf{u}) = -\frac{3}{2} U\mathbf{Q} : \left(\mathbf{uu} - \frac{\mathbf{I}}{3}\right). \tag{21}$$

This potential is derived from an internal energy $E(\mathbf{Q})$ as follows:

$$\Phi = \frac{\partial E(\mathbf{Q})}{\partial \mathbf{Q}} : \left(\mathbf{uu} - \frac{\mathbf{I}}{3}\right) = -\frac{3}{2} U\mathbf{Q} : \left(\mathbf{uu} - \frac{\mathbf{I}}{3}\right) \tag{22}$$

where U has units of energy per unit volume. The entropy per molecule S is

$$TS = -\frac{3}{2} U\mathbf{Q} : \mathbf{Q} + kT \ln Z = 2E + kT \ln Z \tag{23}$$

where the partition function Z is

$$Z = \int e^{-\Phi/k_B T} d\mathbf{u}. \tag{24}$$

Using Equations (22) and (23), the molar free energy A of the system is found to be

$$A = -N_A E - N_A k_B T \ln Z = \frac{3N_A}{4} U\mathbf{Q} : \mathbf{Q} - N_A k_B T \ln Z. \quad (25)$$

Now we check for the thermodynamic consistency. According to thermodynamics the relation between the internal energy E and the free energy A is given by the following expression:

$$E(\mathbf{Q}) = \frac{d\beta A}{d\beta} \quad (26)$$

where $\beta = 1/k_B T$. Using Equations (25) and (26) we find the consistent result:

$$E(\mathbf{Q}) = \frac{d\beta A}{d\beta} = \frac{N_A d}{d\beta}(-\beta E - \ln Z) = \left(-E - \frac{1}{Z}\frac{dZ}{d\beta}\right) = -E + 2E. \quad (27)$$

To find $\mathbf{Q}$ we must minimise A. By minimising the free energy we obtain

$$\frac{dA}{d\mathbf{Q}} = \frac{3}{2} U N_A \mathbf{Q} - N_A k_B T \frac{1}{Z}\frac{dZ}{d\mathbf{Q}} = 0 \quad (28)$$

which yields the self-consistent relation:

$$\mathbf{Q} = \frac{1}{Z}\int \left(\mathbf{uu} - \frac{\mathbf{I}}{3}\right) e^{-\Phi/k_B T} d\mathbf{u}. \quad (29)$$

For a uniaxial LC ($\mathbf{Q} = S(\mathbf{nn} - \mathbf{I}/3)$), contracting Equation (29) with $\mathbf{nn}$ yields

$$S = \frac{1}{Z}\int \frac{3}{2}\left((\mathbf{u}\cdot\mathbf{n})^2 - \frac{1}{3}\right) e^{-\Phi/k_B T} d\mathbf{u}. \quad (30)$$

Appendix II: Orientation distribution function and order parameter for a binary mixture

In this appendix, we derive the orientation distribution function ODF_{mix} for a binary mixture of two discotic nematogens in terms of the single-component distribution functions ODF. The orientation distribution functions and order parameter of a single-component nematic LC were introduced in Equations (1) and (2). Using a mass balance we find that normalised species orientation distribution functions ODF_{mix} are given by

$$\mathrm{ODF}_1(\mathbf{u}) = \frac{\rho_1(\mathbf{u})}{\rho_1}; \quad \mathrm{ODF}_2(\mathbf{u}) = \frac{\rho_2(\mathbf{u})}{\rho_2} \quad (31)$$

where $\mathbf{u}$ is the unit normal to a molecular disc, (ρ_1, ρ_2) are the molar densities and ($\rho_1(\mathbf{u})$, $\rho_2(\mathbf{u})$) are the molar densities at orientation $\mathbf{u}$. Introducing the molar fraction of the two components, $\rho_1 = m_1\rho$, $\rho_2 = m_2\rho$, where ρ is molar density of the mixture, Equations (31) become

$$\mathrm{ODF}_1(\mathbf{u}) = \frac{\rho_1(\mathbf{u})}{m_1\rho}; \quad \mathrm{ODF}_2(\mathbf{u}) = \frac{\rho_2(\mathbf{u})}{(1-m_1)\rho}. \quad (32)$$

Using a mass balance, the normalised orientation distribution function of the mixture is

$$\mathrm{ODF}_{mix}(\mathbf{u}) = \frac{\rho(\mathbf{u})}{\rho} = \frac{\rho_1(\mathbf{u}) + \rho_2(\mathbf{u})}{\rho} \quad (33)$$

where we used the molar density of the mixture with orientation $\boldsymbol{u}$: $\rho(\mathbf{u}) = \rho_1(\mathbf{u}) + \rho_2(\mathbf{u})$. Combining Equations (32) and (33) we find that the $\mathbf{ODF}_{mix}$ is a linear function of the species

$$\mathrm{ODF}_{mix}(\mathbf{u}) = m_1 \mathrm{ODF}_1(\mathbf{u}) + m_2 \mathrm{ODF}_2(\mathbf{u}). \quad (34)$$

Next we define the tensor order parameter of a binary mixture $\mathbf{Q}_{mix}$. We have explained the nature, origin and physical significance of the tensor order parameter $\mathbf{Q}$ of a single component nematic LC in the introduction (Equation (2)). Multiplying Equation (34) with $(\mathbf{uu} - \boldsymbol{\delta}/3)$ and integrating on the unit sphere we find

$$\int \mathrm{ODF}_{mix}(\mathbf{u})(\mathbf{uu} - \boldsymbol{\delta}/3) d^2\mathbf{u} = m_1 \int \mathrm{ODF}_1(\mathbf{u})(\mathbf{uu} - \boldsymbol{\delta}/3) d^2\mathbf{u} + m_2 \int \mathrm{ODF}_2(\mathbf{u})(\mathbf{uu} - \boldsymbol{\delta}/3) d^2\mathbf{u}. \quad (35)$$

Using Equations (2) and (35), we finally arrive at $\mathbf{Q}_{mix}$:

$$\mathbf{Q}_{mix} = m_1 \mathbf{Q}_1 + m_2 \mathbf{Q}_2. \quad (36)$$